DAV International Journal of Science

EFFECT OF ANNEALING ON STRUCTURAL AND MAGNETIC PROPERTIES OF IRON OXIDE NANOPARTICLES

Shahane G. S.
Department of Electronics,
DBF Dayanand College of Arts and Science, Solapur, MS, India
Email: shahanegs@yahoo.com

ABSTRACT
Nanocrystalline Fe_3O_4 particles were synthesized by a facile chemical route and annealed at different temperatures in argon atmosphere. The material is then characterized by X-ray diffraction technique (XRD) and dc magnetization measurements. The X-ray diffraction patterns confirm the synthesis of single crystalline phase of Fe_3O_4 nanoparticles. On annealing at 300°C there is improvement in the crystal structure. A phase transition from magnetite (Fe_3O_4) to hematite (α-Fe_2O_3) is observed when the samples are annealed above 500°C. The magnetic measurements show superparamagnetic nature of the as-synthesized sample, whereas for annealed samples ferromagnetic nature is observed. The saturation magnetization decreases after phase transition.

KEY WORDS: Fe_3O_4 nanoparticles, structural characterization, phase transition, magnetic properties

INTRODUCTION

In recent years, ferrite nanoparticles have gained scientific and technological importance due to their excellent magnetic properties suitable for a broad range of applications. Various interesting phenomena such as superparamagnetisim, spin canting, core/shell structure, metastable cation distribution, etc. are observed in nanoparticles of ferrites (Caruntu *et al.* 2007). Among the various nanocrystalline ferrites, Fe_3O_4 has attracted particular interest as an ideal candidate for different biomedical applications such as cell separation, magnetic resonance imaging, enzyme encapsulation, gene and radionuclide delivery, tumor hyperthermia and targeted drug delivery (Sahoo *et al.* 2005; Zaho *et al.* 2008). The properties of ferrites are found to be influenced by the method of preparation, deposition conditions and post deposition treatment. Variety of methods has been developed for the synthesis of ferrite nanoparticles. These include sol-gel, hydrothermal, chemical co-precipitation, sonochemical reactions and ball milling (Cao *et al.* 2005). However, chemical co-precipitation method is relatively simple and provides good control over particle properties. This paper presents synthesis of Fe_3O_4 nanoparticles by chemical co-precipitation method and reports the effect of annealing on some of its properties.

MATERIALS AND METHODS

Fe_3O_4 nanoparticles were prepared by the chemical co-precipitation method (Shahane *et al.* 2010). The starting materials were $FeCl_2$ and $FeCl_3$ (all AR grade). For synthesis, equimolar solutions of $FeCl_2$ and $FeCl_3$ were mixed in their stoichiometric ratio and homogenized at room temperature. The pH of the solution was adjusted by adding ammonia solution. The mixture was then heated at 80 °C for about one hour. Oleic acid was used as surfactant to prevent agglomeration of particles. The precipitate was then washed several times with double distilled water to remove the salt residues and other impurities. The samples were annealed at 300°C, 500°C and 700°C in argon atmosphere for one hour. These samples were then characterized through various characterization techniques.

The X-ray diffraction patterns (XRD) were recorded using a Rigaku powder X-ray diffractometer with Cu K_α (λ=1.54059 Å) radiation. The scanning was done in the 2θ range from 20° to 70° at a scanning speed of 0.02°/s. The magnetization measurements were carried out on these samples by a search coil method. A polytronic power supply (Model- BCS-1000), electromagnet (Type Hem-100) and flux meter (Model FM109) were used for this purpose. The setup was calibrated using the standard nickel sample.

RESULTS AND DISCUSSION

The structural analysis of samples was done by powder X-ray diffraction technique using CuK_α radiation. Fig. 1 show the powder X-ray diffraction patterns for as-synthesized and annealed samples. The detail XRD analysis is given in Table 1. From Table 1 it is seen that the 'd' values and intensities of the observed diffraction peaks match with the single crystalline spinel form of Fe_3O_4 nanoparticles (JCPDS Card No. PDF #00-019-0629). The discernible peaks at 2θ values 30.12, 35.54, 43.08, 57.06 and 62.72 can be indexed to (220), (311), (400), (422), (511) and (440) reflections, respectively. X-ray diffraction pattern (Fig. 1 a) shows broad peaks indicating ultrafine nature and small crystallite size of the particles. The lattice parameters were calculated for these samples. It is observed that lattice parameter is 8.4090 Å. On annealing at 300°C there is improvement in sharpness of the peaks, however, no change in peak positions is

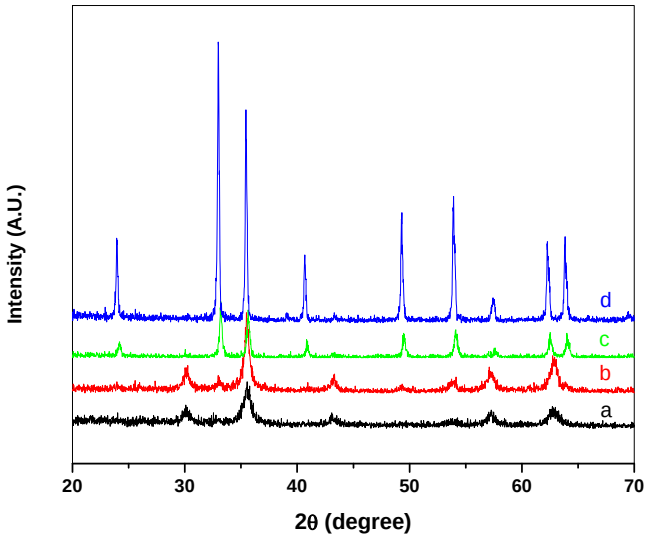

Fig. 1 X-ray diffractograms of as-synthesized and annealed samples: (a) raw, (b) 300°C, (c) 500°C and (d) 700°C.

Table 1: XRD analysis of as-synthesized and annealed samples

Annealing temperature (°C)	Peak No.	2θ deg.	d_{obs} Å	d_{JPCD} Å	I/I_{max} (obs.)	I/I_{max} (JPCD)	(hkl) planes	Observed Phase
Raw	1	30.12	2.9649	2.9670	30	30	(220)	Fe_3O_4
	2	35.54	2.5239	2.5320	100	100	(311)	
	3	43.08	2.0978	2.0993	20	20	(400)	
	4	57.06	1.6128	1.6158	25	30	(511)	
	5	62.72	1.4802	1.4845	35	40	(440)	
300	1	30.12	2.9649	2.9670	30	30	(220)	Fe_3O_4
	2	35.48	2.5280	2.5320	100	100	(311)	
	3	43.32	2.0869	2.0993	20	20	(400)	
	4	57.01	1.6142	1.6158	25	30	(511)	
	5	62.74	1.4797	1.4845	35	40	(440)	
500	1	24.14	3.6838	3.6840	30	30	(012)	α-Fe_2O_3
	2	33.20	2.6962	2.7000	100	100	(104)	
	3	35.52	2.5255	2.5190	75	70	(110)	
	4	40.84	2.2084	2.2070	27	20	(113)	
	5	49.48	1.8406	1.8406	40	40	(024)	
	6	54.12	1.6933	1.6941	45	45	(116)	
	7	57.54	1.6007	1.6033	10	05	(112)	
	8	62.52	1.4844	1.4859	30	30	(214)	
	9	64.00	1.4536	1.4538	30	30	(300)	
700	1	24.00	3.7051	3.6840	30	30	(012)	α-Fe_2O_3
	2	33.06	2.7075	2.7000	100	100	(104)	
	3	35.44	2.5313	2.5190	75	70	(110)	
	4	40.68	2.216	2.2070	27	20	(113)	
	5	49.32	1.8463	1.8406	40	40	(024)	
	6	53.92	1.6993	1.6941	45	45	(116)	
	7	57.40	1.6041	1.6033	10	05	(112)	
	8	62.28	1.4896	1.4859	30	30	(214)	
	9	63.84	1.4569	1.4538	30	30	(300)	

observed (Fig. 1b). Further annealing at 500°C (Fig. 1c) show peaks at 2θ values 24.14, 33.2, 35.52, 40.84, 49.48, 54.12, 57.54, 62.52 and 64.00 which can be indexed as (012), (104), (110), (113), (024), (116), (112), (214) and (300) reflections of α-Fe_2O_3, respectively (JCPDS Card No. PDF #00-033-0664). No peaks corresponding to Fe_3O_4 are observed. Increase in annealing temperature further to 700°C increases the peak intensities without much affecting the peak position (Figure 1d). This clearly shows that on annealing at 500°C there is a phase transition from cubic spinel Fe_3O_4 to more stable hexagonal α-Fe_2O_3 structure. Lattice parameters for both the structures are listed in Table 2.

The crystallite size of as-synthesized and annealed samples was then determined from the broadening of the respective high intensity peak by using the Scherer relation:

$$D = 0.89\,\lambda / \beta \cos\theta \qquad \text{--- (1)}$$

where, D is the crystallite size, λ is wavelength of X-ray, β is full width at half maximum (FWHM) measured in radians and θ is the Bragg angle. The calculated values are listed in Table 2. It is observed that the average crystallite size increases as annealing temperature increases. The increase in the crystallite size after annealing indicates the grain growth of the particles at the temperature well below the melting temperature of the bulk ferrites (Shahane *et al*. 2010).

Magnetic measurements were carried out on these samples and Fig. 2 displays the magnetization curves for these samples. The magnetization curve demonstrates a typical superparamagnetic behavior of the as-synthesized sample.

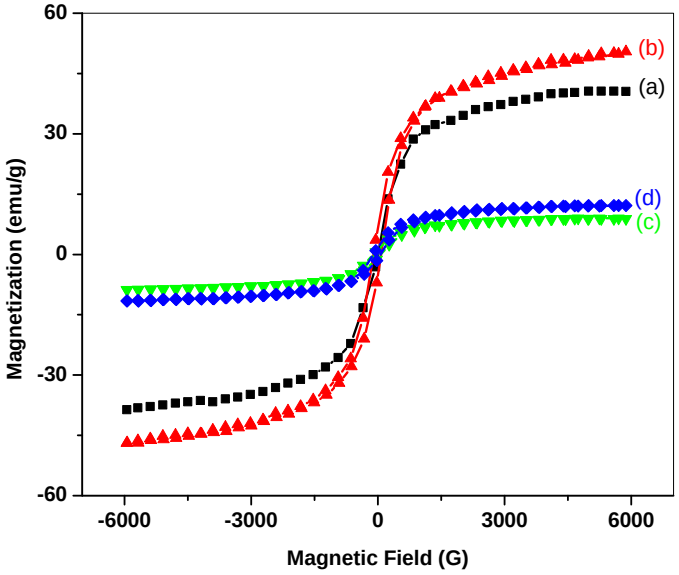

Fig. 2 Magnetization curves for as-synthesized and annealed samples: (a) raw, (b) 300°C, (c) 500°C and (d) 700°C.

The superparamagnetism of these nanoparticles can be attributed to their fine crystallite size, which makes it easier for them to be thermally activated to overcome the magnetic anisotropy (Zhao *et al.* 2006). It is seen that saturationmagnetism is 40.5emu/g. The smaller value of saturation magnetization as compared to bulk value is due to lattice defects, weaker magnetic superexchange interactions between A-sites and B-sites, and random orientation of spin on the surface of the nanoparticles (Caruntu *et al.* 2007; Priyadarshni *et al.* 2009, Rao *et al.* 2006). On annealing at 300°C the curve shows hysteresis indicating ferromagnetic nature of the sample. The saturation magnetization also increases. This can be attributed to the larger crystallite size of the sample. The values of saturation magnetization, remenance and coercivity are listed in Table 2. For samples annealed at 500°C and 700°C curves show hysteresis, however a very small magnetization is observed. The decrease in saturation magnetization can be attributed to phase transition from Fe_3O_4 to α-Fe_2O_3 phase when annealed above 500°C. Fe_3O_4 (magnetite) is ferrimagnetic in nature whereas, α-Fe_2O_3 (hematite) is antiferromagnetic in nature which shows poor magnetism. Thus magnetization decreases after phase transition.

Table 2: Structural and magnetic parameters of as-synthesized and annealed samples

Annealing Temperature (^oC)	Lattice Parameter (Å)	Crystallite Size (nm)	Saturation Magnetization (emu/g)	Remanence (emu/g)	Coercivity (G)
Raw	a = 8.3708	12	42	0	0
300	a = 8.3844	22	51	7	105
500	a =5.03195 c =13.7270	42	9	1.5	100
700	a = 5.04684 c = 13.7957	61	12	2	100

CONCLUSION

A low temperature chemical co-precipitation method is used for synthesis of nanocrystalline Fe_3O_4 particles. The X-ray diffraction pattern confirms the synthesis of single crystalline phase of Fe_3O_4 nanoparticles. On annealing at 300^{o}C there is improvement in the crystal structure. A phase transition from magnetite (Fe_3O_4) to hematite (α-Fe_2O_3) is observed when the samples are annealed above 500^{o}C. The magnetic measurements show superparamagnetic nature of the as-synthesized sample, whereas for annealed samples ferromagnetic nature is observed. The saturation magnetization decreases after phase transition.

REFERENCES

Caruntu D, Caruntu G. and O'Connor C. J. (2007). Magnetic properties of variable- sized Fe_3O_4 nanoparticles synthesized from non-aqueous homogeneous solutions of pylols. *J. Phys. D: Appl. Phys.* **40:** 5801-5809.

Cao X and Gu L. (2005). Spindly cobalt ferrite nanocrystals: preparation, characterization and magnetic properties. *Nanotechnology* **16:**180-185.

Priyadarshni P., Pradeep A. and Chandrasekaran G. (2009). Novel combustion route of synthesis and characterization of nanocrystalline mixed ferrites of Ni-Zn. *J. Magn. Magn. Mater.* **321:** 1898-1903.

Rao B. P. and Caltun O. F. (2006). Synthesis and characterization of some ferrite nanoparticles. *J. Optoelectr. and Adv. Mater.* **8 (3):** 991-994.

Sahoo Y., Goodarzi A., Swihart M. T., Ohulchanskyy T. Y., Kaur N., Furlani E. P. and Prasad P.N. (2005). Aqueous ferrofluid of magnetite nanoparticles: Fluorescence labeling and magnetophoretic control. *J. Phys. Chem. B* **109:** 3879-3885.

Shahane G.S., Ashok Kumar, Arora M., Pant R.P. and Krishan Lal (2010). Synthesis and characterization of Ni–Zn ferrite nanoparticles. *J. Magn. Magn. Mater.* **322:**1015-1019.

Zhao S. Y., Lee D. K., Kim C. W., Cha H. G., Kim Y. H. and Kang Y. S. (2006). Synthesis of magnetic nanoparticles of Fe_3O_4 and $CoFe_2O_4$ and their surface modification by surfactant adsorption. *Bull. Korean Chem. Soc.* **27(2):** 237-242.

Zhao Y., Zumin Q and Jiaying H. (2008). Preparation and analysis of Fe_3O_4 magnetic nanoparticles used as targeted-drug carriers. *Chin. J. Chem. Engin.*, **16(3)**: 451-455.